Calcium Binding Sites of Calmodulin and Electron Transfer by Neuronal Nitric Oxide Synthase†

Regina Stevens-Truss,‡ Kathy Beckingham,§ and Michael A. Marletta*,‡,||,⊥

Interdepartmental Program in Medicinal Chemistry, College of Pharmacy, and Department of Biological Chemistry, School of Medicine, University of Michigan, Ann Arbor, Michigan 48109-1065, and Howard Hughes Medical Institute and Department of Biochemistry and Cell Biology, Rice University, Houston, Texas 77251

Received April 25, 1997; Revised Manuscript Received July 25, 1997⊗

ABSTRACT: Although binding of calmodulin (CaM) to neuronal nitric oxide synthase (nNOS) has been demonstrated to act as the trigger necessary for electron transfer and catalytic activity, the exact manner in which this is achieved is unclear. By using a series of single point mutants of *Drosophila melanogaster* CaM, the role that each Ca^{2+} binding site plays in the transfer of electrons within nNOS has been examined. In these mutants, the bidentate glutamic acid (E) residue which coordinates Ca^{2+} at the −Z position in each site has been mutated to a glutamine (Q), preventing Ca^{2+} binding at that site. The results demonstrate that Ca^{2+} binding at site I of CaM is critical for all electron transfer reactions. All nNOS activities measured (citrulline formation, NADPH oxidation, and cytochrome *c* reduction) in the presence of the site I CaM mutant (denoted B1Q) were only 2% of the nNOS activity with wild-type CaM. The B2Q and B4Q mutants activated nNOS to similar levels. These two mutants, however, affected nNOS heme-dependent activities to a greater extent than they affected activities independent of the nNOS heme. The site III CaM mutant (B3Q) activated nNOS to levels similar to activities measured with wild-type CaM. Rates of formation of the ferrous−CO complex were also obtained with each of the mutant CaMs. The relative binding affinities of these mutants do not correlate with the observed differences in electron transfer rates. These results demonstrate that, although binding of CaM to nNOS is necessary for catalysis, specific interactions between the two proteins exist which are required for efficient electron transfer.

In the last decade, nitric oxide (·NO)[1] has emerged as an important regulator of physiological functions. The enzyme nitric oxide synthase (NOS, EC 1.14.13.39) catalyzes the conversion of L-arginine to citrulline and ·NO. The reaction requires O_2 and NADPH, and proceeds via the intermediate N^G-hydroxy-L-arginine (*1*−*3*). Three distinct isoforms of NOS have been characterized and have been classified as either constitutive or inducible, depending on their mode of regulation. The activity of the constitutive isoforms (which include the neuronal and endothelial isoforms) is regulated by the reversible binding of CaM in a classical Ca^{2+}-dependent fashion. The inducible isoform (e.g., that isolated from murine macrophages) is transcriptionally regulated by the action of cytokines, and copurifies with CaM as a tightly bound subunit in an apparently Ca^{2+}-independent manner (*4*). All isoforms of NOS isolated to date are homodimers. Each subunit binds one protoporphyrin IX heme, with spectral characteristics similar to those of cytochrome P450 (*5*−*7*), 1 equiv each of FMN and FAD (*8*−*10*), and (6*R*)-tetrahydro-L-biopterin (H_4B) (*9, 11, 12*).

The structure of nNOS can be schematically represented as depicted in Figure 1. In this model, the enzyme is separated into two functional domains, an N-terminal heme domain and a C-terminal reductase domain, separated by the putative CaM binding sequence. The relative location of the cofactors, as indicted in Figure 1, is supported by several experimental findings. Bredt and colleagues (*13*) identified amino acid residues in the C-terminus of neuronal NOS (nNOS) for flavin and NADPH binding by sequence comparison to the NADPH−cytochrome P450 reductases. Recently, McMillan and Masters (*14*) reported the bacterial expression of the C-terminal half of nNOS (residues 715−1429), and demonstrated that this portion of the nNOS sequence contains the bound flavins. They also demonstrated that this portion of nNOS possesses cytochrome *c* reductase activity comparable to the full-length enzyme, indicating that this function of nNOS is mediated via the flavins. Several studies have identified the thiolate of cysteine 415 as the probable axial heme ligand (*15, 14, 12*). The partially purified *E. coli* expressed hemoprotein (residues 1−714 of nNOS), in fact, exhibits the typical cytochrome P450 spectral shift caused by the formation of the reduced iron−CO complex, and also binds L-arginine and H_4B (*14*). Support

† We gratefully acknowledge the NIH (CA50414 to M.A.M. and GM49155 to K.B.), C-1119 Welch Foundation to K.B., and a UNCF•Merck Research Fellowship (to R.S.-T.) for financial support.

* To whom correspondence should be addressed at the College of Pharmacy, 428 Church St., University of Michigan, Ann Arbor, MI 48109-1065.

‡ Interdepartmental Program in Medicinal Chemistry, University of Michigan.

§ Department of Biochemistry and Cell Biology, Rice University.

|| Department of Biological Chemistry, School of Medicine, University of Michigan.

⊥ Howard Hughes Medical Institute.

⊗ Abstract published in *Advance ACS Abstracts,* September 15, 1997.

[1] Abbreviations: NOS, nitric oxide synthase; nNOS, rat neuronal nitric oxide synthase; CaM, calmodulin; H_4B, (6*R*)-5,6,7,8-tetrahydro-L-biopterin; HEPES, 4-(2-hydroxyethyl)piperazineethanesulfonic acid; BSA, bovine serum albumin; DTT, dithiothreitol; TCA, trichloroacetic acid; EGTA, ethylene glycol bis(β-aminoethyl ether)-*N*,*N*,*N*′,*N*′-tetraacetic acid; EDTA, ethylenediamine-*N*,*N*,*N*′,*N*′-tetraacetic acid; SDS−PAGE, sodium dodecyl sulfate−polyacrylamide gel electrophoresis; PVDF, poly(vinylidene difluoride); TnC, troponin C; MLCK, myosin light chain kinase. Mutant CaM nomenclature: B*x*Q, B*x* denotes the Ca^{2+} binding site, and Q denotes the substituted residue (glutamine).

S0006-2960(97)00973-2 CCC: $14.00

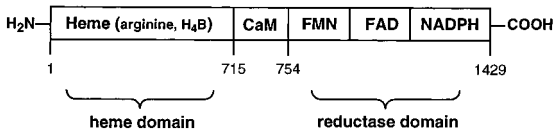

FIGURE 1: Schematic representation of the nNOS primary sequence, showing binding regions of the various functional groups. Amino acid residue positions are indicated by numbers. This schematic is based on work cited in the introduction.

for the putative CaM binding site comes from studies using synthetic peptides; indeed, peptides corresponding to residues 715−754 (*16*−*18*) bind CaM with affinities (low nanomolar) similar to that of the full-length enzyme (*19*).

Reduction of the NOS heme is required for catalysis. Binding of CaM has been demonstrated to be essential for efficient electron transfer and catalytic activity of nNOS (*20*, *21*). CaM also increases the rate at which nNOS reduces cytochrome *c* (*12*, *21*). In this fashion, CaM serves a dual function in that it regulates electron transfer (i) from the flavins to the heme of nNOS (representing intramolecular electron transfer) and (ii) to an exogenous electron acceptor such as the heme of cytochrome *c* (representing intermolecular electron transfer). The role that CaM plays in affecting these two functions is not clear. Binding and activation of target proteins by CaM typically require occupancy of the four Ca^{2+} binding sites of CaM [for recent reviews, see (*22*, *23*)]. The crystal structure of the Ca^{2+}-saturated form of CaM shows that the protein adopts a dumbbell-like structure, with each lobe composed of two EF-hands (helix−loop−helix motif) separated by a central linker (*24*, *25*); a schematic representation of the amino acid sequence of CaM is shown in Figure 2. This central linker functions in solution as a flexible tether between the two terminal lobes (*26*). In most cases, including nNOS, the target binding structure of CaM is generated upon Ca^{2+} binding. The carboxy-terminal lobe contains the two high-affinity Ca^{2+} sites (sites III and IV), while the amino-terminal lobe contains the two sites with lower Ca^{2+} affinity (sites I and II). It has been demonstrated that the major conformational changes that CaM undergoes upon Ca^{2+} binding occur when sites III and IV are occupied (*27*, *28*).

The role that Ca^{2+} binding to CaM plays in CaM's actions on various target enzymes has been investigated. A series of single point mutants of *Drosophila* CaM have been generated by changing the conserved bidentate glutamate residue, critical for Ca^{2+} coordination in each EF-hand, to a glutamine (see Figure 2) (*29*), causing an impaired ability of Ca^{2+} to bind to the mutated site. Studies with these mutants have revealed that the binding of CaM to target proteins does not necessarily lead to activation of the target, but rather that target activation requires specific, Ca^{2+}-dependent interactions between the two proteins (*30*, *31*). Since CaM has been demonstrated to regulate intramolecular and intermolecular electron transfer in nNOS, the present study was designed to examine the role that each Ca^{2+} binding site of CaM plays in these reactions. In addition, a CaM with all four Ca^{2+} binding sites carrying the E to Q mutation, termed B1234Q (*32*), has been studied. The results demonstrate that, as for other CaM-activated enzymes, nNOS is not activated by CaM binding alone. Our data show that there are interactions between regions of CaM and nNOS that are required for electron transfer within the reductase domain of nNOS. The data also demonstrate that separate

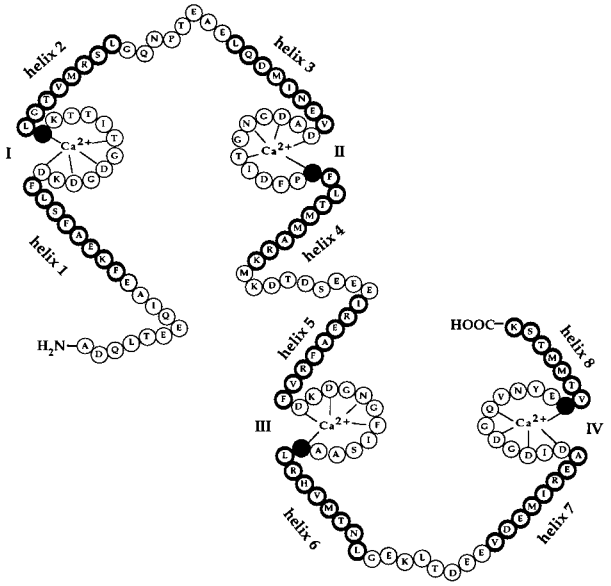

FIGURE 2: Amino acid sequence of calmodulin. The sequence of *Drosophila* calmodulin is shown, using single-letter amino acid residue codes. The amino acid residues which make up each Ca^{2+} binding site, indicated by Roman numerals, are shown in a pocket-like configuration. Amino acid residues contained in boldface circles indicate stretches of α-helices. The filled circle in each Ca^{2+} binding site corresponds to the residue mutated from glutamate (E) to glutamine (Q). When that residue is glutamate, Ca^{2+} binds at the site, but when glutamine is at that position, Ca^{2+} binding is essentially eliminated. Each Ca^{2+} binding site, in combination with its two adjacent helices, makes up an EF-hand of calmodulin: helix 1 + Ca^{2+} binding site I + helix 2 make up EF-hand 1; helix 3 + Ca^{2+} binding site II + helix 4 make up EF-hand 2; and so on. In the Ca^{2+}-bound dumbbell structure, EF-hands 1 and 2 are part of the amino-terminal lobe while EF-hands 3 and 4 are part of the carboxy-terminal lobe.

interactions between CaM and nNOS are responsible for electron transfer within the heme domain. We propose a structural representation of the interactions between CaM and nNOS which may help explain how CaM affects both electron transfer pathways.

EXPERIMENTAL PROCEDURES

Materials and General Methods. *Spodoptera frugiperda* (Sf9) cells were obtained from American Type Culture Collection (ATCC, CRL 1711) and maintained as previously described (*15*) in Grace's insect cell culture medium (Gibco BRL), supplemented with 10% fetal bovine serum (HyClone Laboratories, Inc.) and 1% antibiotic solution (Sigma, #A 9909). All tissue culture flasks were purchased from Corning and Costar. H_4B was purchased from Dr. B. Schircks Laboratory (Jona, Switzerland) and prepared in 15 mM HEPES (pH 7.5) containing 100 mM DTT. 2′,5′-ADP−Sepharose 4B and CaM−Sepharose 4B were from Pharmacia−LKB Biotechnology, Inc. Bradford protein dye reagent was from Bio-Rad. L-[U-^{14}C]Arginine (specific activity = 319 mCi/mmol) was purchased from Amersham Corp. [^{125}I]-CaM was from DuPont (specific activity = 133 μCi/μg). Ecolume scintillation cocktail was from ICN-Flow. Matheson-purity carbon monoxide (99.99%) and prepurified argon (99.998%) were purchased from Matheson Gas Products. Bovine CaM and all other reagents, unless otherwise noted, were obtained from Sigma Chemical Co.

Expression and Purification of nNOS. Sf9 cells were infected with wild-type recombinant virus as described previously (*12*, *15*) and harvested 72 h later. The 100000*g* supernatant was stored at −80 °C. Purification procedures were as previously reported (*12*) with the following modifications: the 100000*g* supernatant [1000−2000 units; 1 unit = 1 nmol of ·NO/min as measured by the oxyhemoglobin oxidation assay (*33*)] was applied to a 2′,5′-ADP−Sepharose 4B column (1.5 g) which had been equilibrated with buffer A (50 mM HEPES, 0.5 mM arginine, 100 mM NaCl, and 10% glycerol at pH 7.5). The column was then washed with 10 mL of buffer A containing 0.1 mM EDTA and 0.1 mM EGTA, followed by a 20 mL wash consisting of the same components with the addition of 200 mM NaCl. Following a 20 mL wash with buffer B (50 mM HEPES, 100 mM NaCl at pH 7.5), nNOS was eluted with 30 mL of buffer B containing 2 mM $CaCl_2$ and 5 mM NADPH directly onto a 2 mL CaM affinity column (made by mixing 2 mL of CaM−Sepharose 4B with 2 mL of Sepharose 4B resin) which had been preequilibrated with buffer B containing 2 mM $CaCl_2$. The column was washed with 10 mL of buffer B containing 2 mM $CaCl_2$, and nNOS was eluted with 15 mL of buffer C (50 mM HEPES, 100 mM NaCl, and 10% glycerol at pH 7.5) containing 5 mM EGTA. nNOS was eluted directly into an ultrafiltration cell (Amicon) and concentrated 15-fold using a 70 kDa molecular mass cutoff membrane (Filtron). The elution buffer was exchanged with 10 mL of buffer C during the concentration step. H_4B (10 μM) was included throughout the purification and concentration steps. Purified nNOS was stored at −80 °C in the presence of 20% glycerol and 10 μM H_4B. nNOS purified in this fashion yielded protein which was deemed greater than 95% pure by SDS-PAGE stained with Coomassie Blue R-250.[2] The specific activity of the purified nNOS was typically between 500 and 800 nmol min^{-1} mg^{-1}. Protein concentrations were determined by Bradford microassay using BSA as the standard and an nNOS molecular mass of 160 kDa.

Expression and Purification of CaM. Mutant and wild-type *Drosophila* CaM were prepared as previously described (*29*, *32*), and their concentrations were determined using previously reported extinction coefficients (*29*). Bovine CaM was purchased from Sigma and prepared as a 1 mg/mL solution. All CaM solutions were stored at −20 °C.

Activity Assays. The activity of nNOS was determined using the citrulline assay as previously described (*33*), with the following modifications: Reaction mixtures (300 μL) containing nNOS (30−35 nM), L-[U-^{14}C]arginine (100 μM, specific activity = 3 μCi/μmol), H_4B (25−50 μM), DTT (300−600 μM), glycerol (0.17%), $CaCl_2$ (1.2 mM), CaM (concentrations ranging from 0 to 300 nM), and HEPES (100 mM, pH 7.5) were initiated with NADPH (200 μM) and allowed to proceed for 5 min at 37 °C. The reactions were terminated, and unreacted arginine was separated from citrulline as described previously (*34*). nNOS activity was also determined by the hemoglobin assay as described in Hevel and Marletta (*33*) with the following modifications: nNOS (1.8−2 μM) was incubated with wild-type *Drosophila* CaM (2.93 μM) and $CaCl_2$ (1.2 mM), and kept on ice prior to being assayed. Aliquots (10 μL) were then assayed (500 μL assay volume) at 37 °C in the presence of varying concentrations of mutant CaM. Assays were initiated with NADPH (60 μM). Activities were calculated using an extinction coefficient of 60 000 M^{-1} cm^{-1} for the increase in absorbance at 401 nm, indicative of methemoglobin production.

NADPH oxidation catalyzed by nNOS in the presence of the various CaMs was measured as described in Richards *et al.* (*12*) with the following modifications: Assays contained nNOS (40−80 nM), H_4B (15 μM), DTT (200 μM), $CaCl_2$ (1 mM), NADPH (120 μM), and HEPES (100 mM, pH 7.5) at 37 °C in a final volume of 500 μL. Assays were initiated with CaM (150 nM), and monitored by following the decrease in absorbance at 340 nm. Activity was determined using a $\Delta\epsilon$ of 6200 M^{-1} cm^{-1}. NADPH oxidase activity of wild-type and C415A[2] mutant nNOS in the presence of cytochrome *c* was measured as follows: Assays containing nNOS (8−10 nM), $CaCl_2$ (1 mM), CaM (150 nM), cytochrome *c* (50 μM), and HEPES (100 mM, pH 7.5) at 37 °C in a final volume of 500 μL were initiated with NADPH (30 μM) and monitored at 337.5 nm. This wavelength was chosen because reduction of cytochromes *c* causes a decrease in absorbance at 340 nm which overestimates NADPH oxidation values. Oxidized and reduced cytochrome *c*, however, have an isosbestic point at 337.5 nm. Activity was determined using a $\Delta\epsilon$ of 6200 M^{-1} cm^{-1}.

Cytochrome *c* reduction catalyzed by nNOS in the presence of the various CaMs was measured as described in Richards *et al.* (*12*) with the following modifications: Assays contained nNOS (10−20 nM), $CaCl_2$ (1 mM), NADPH (120 μM), CaM (300 nM), cytochrome *c* (50 μM), and HEPES (100 mM, pH 7.5) at 37 °C, in a final volume of 500 μL. Assays were monitored at 550 nm, and activity was determined using a $\Delta\epsilon$ of 21 000 M^{-1} cm^{-1}.

Formation of the Ferrous−CO Complex. UV−Visible spectra were obtained on a Cary 3E spectrophotometer equipped with a Neslab RTE-111 circulating water bath. All spectral experiments were carried out at 4 °C, unless otherwise stated, using a specially designed anaerobic cuvette as previously described (*35*). Samples (400 μL) of nNOS (1.8−4.2 μM) in 50 mM HEPES (pH 7.5) with glycerol (10−20%), NaCl (50−100 mM), H_4B (5−10 μM), and $CaCl_2$ (1.25 mM) were placed in the anaerobic cuvette and kept on ice while the headspace was equilibrated with CO for 15 min. Following this equilibration step, NADPH (25−35 μM) which had been flushed with argon was added to the nNOS sample using a Hamilton gas-tight syringe. Spectra were recorded every 2 min for 20−30 min. CaM (2−5 μM) which had been flushed with argon was then added to the cuvette using a Hamilton gas tight syringe, and spectra were recorded every 2 min for 60−120 min.

Spectral Determinations of Arginine Binding. Spectra were obtained at 4 °C, as described above. nNOS (1−2 μM) in 400 μL of 50 mM HEPES (pH 7.5) with glycerol (10%), NaCl (50 mM), H_4B (5 μM), and $CaCl_2$ (1.25 mM) was placed in a quartz cuvette, either in the absence or in the presence of the various CaMs (2−3 μM), and the spectrum was recorded. Concentrations of arginine varying from 0 to 20 μM were added to the cuvette, and the spectrum was recorded after each addition to determine if the various CaMs affected substrate binding.

[2] The C415A mutant nNOS was expressed using a baculovirus/Sf9 cell system (*12*). Purification was as described here for wild-type nNOS except that no arginine or H_4B was added to the buffers. The purified enzyme was stored at −80 °C in the absence of H_4B.

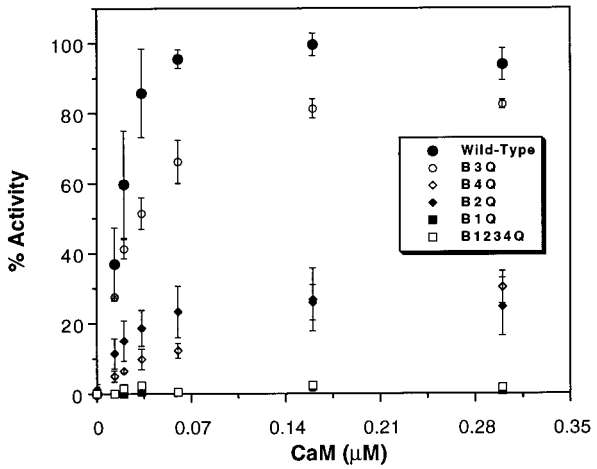

FIGURE 3: Rates of citrulline formation as a function of *Drosophila* CaM concentration. Assays contained nNOS, L-arginine (100 μM), NADPH (200 μM), H_4B (50 μM), and $CaCl_2$ (1.2 mM) in HEPES (100 mM, pH 7.5) as described under Experimental Procedures. Data points represent the average of two experiments performed in duplicate; the error bars represent the standard deviation.

Binding Interaction of CaM with nNOS. nNOS binding to the various CaMs was determined as follows: nNOS (50 nM) in buffer A (50 mM HEPES, 1−1.25 mM $CaCl_2$, pH 7.4) was incubated with ^{125}I-CaM (119 nM and 179 nM, specific activity = 36−144 μCi/μmol) and unlabeled CaM (concentrations ranging from 0 to 20 μM) for 30 min at 4 °C. To the 200 μL assay volume was added 100 μL (dry volume) of 2′,5′-ADP−Sepharose 4B resin. Samples were mixed, and bound from free ^{125}I-CaM was separated by vacuum filtration. nNOS−CaM complex bound to the ADP resin was collected onto 0.45 μm filters, washed with buffer A (3 mL), and counted. Data were analyzed by Dixon plots using KaleidaGraph v.3.0.4 (Abelbeck Software), and the relative affinities of each CaM were then determined.

RESULTS

Activities of nNOS in the Presence of Wild-Type and Mutant CaMs. The ability of nNOS to form citrulline in the presence of the various CaMs was determined. In the presence of *Drosophila* wild-type CaM, nNOS was able to form citrulline at an essentially identical rate as in the presence of bovine CaM (data not shown). As can be seen in Figure 3, the rate of citrulline formation increased in a CaM concentration-dependent fashion. The maximal rate obtained with wild-type CaM was 250-fold faster than that obtained in the absence of CaM (1.2 nmol min^{-1} mg^{-1}). However, in the presence of the various CaM mutants, the rate of citrulline formation was decreased relative to the activity in the presence of wild-type CaM. Figure 3 shows the activity of nNOS in the presence of the various *Drosophila* CaMs, as a percent of the maximal activity obtained with *Drosophila* wild-type CaM (256.4 nmol min^{-1} mg^{-1}). Of the five mutant CaMs examined, the B3Q mutant was the best activator of nNOS at every concentration measured, with activity reaching a maximum of 82%. The B2Q mutant activated to a maximum of 26%, while the B4Q mutant activated to 30%. The B1Q and B1234Q mutants activated to approximately 2% of the wild-type rate.

NADPH oxidation in the absence of an exogenous electron acceptor was also measured. NADPH donates electrons to reduce the nNOS flavins which in turn reduce the heme, as illustrated in Scheme 1. Catalytic consumption of NADPH is dependent on the reoxidation of the heme by O_2; it has been demonstrated that mutant nNOS without heme does not oxidize NADPH (*12*). Wild-type CaM increased the rate of NADPH oxidation 100-fold above the rate observed in the absence of CaM (Table 1). The relative effects of the mutant CaMs on this function were the same as those observed for the formation of citrulline, and are given in Table 1. As with citrulline formation, the B3Q mutant was the best at increasing this activity, activating nNOS to 45% of the wild-type CaM rate. The B2Q and B4Q mutants activated to similar levels (15% of wild-type). The B1Q mutant was the poorest activator, increasing this activity to 2% of the wild-type CaM rate (Table 1). The B1234Q mutant activated to the same level as the B1Q mutant.

Scheme 1: Summary of NOS Electron Transfer Reactions[a]

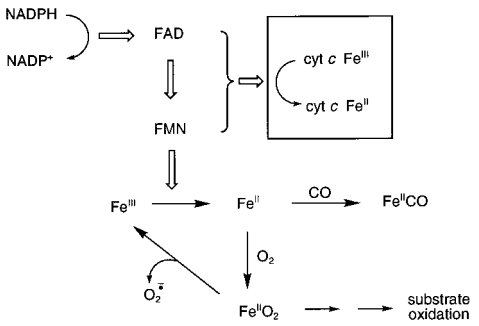

[a] Electron transfer steps are represented by open arrows (⟹). The boxed area around cytochrome *c* serves to represent intermolecular electron transfer.

Table 1: NADPH Oxidation in the Absence of Cytochrome *c*

CaM	activity[a] (nmol min^{-1} mg^{-1})[b]	CaM	activity[a] (nmol min^{-1} mg^{-1})[b]
control	12.1 ± 3.6	B2Q	166.1 ± 19.7
bovine (WT)	1056.3 ± 85.1	B3Q	507.7 ± 48.3
wild-type	1124.0 ± 102.2	B4Q	171.0 ± 33.7
B1Q	22.8 ± 6.7	B1234Q	20.6 ± 9.4

[a] Assays contained nNOS (40−80 nM) and CaM (150 nM), as described under Experimental Procedures. [b] Values are the average of two or more experiments, each performed in duplicate. Errors are the standard error of the means. Control represents nNOS activity in the absence of CaM. Wild-type and B*x*Q CaMs are from *Drosophila*.

nNOS activity in the presence of cytochrome *c* was also measured. In the presence of cytochrome *c*, catalytic consumption of NADPH is dependent primarily on the nNOS flavins (*12, 36*), as illustrated in Scheme 1. NADPH consumption was monitored indirectly as the reduction of cytochrome *c*, and directly as the oxidation of NADPH. The relative rates of cytochrome *c* reduction are given in Table 2. Wild-type CaM increased nNOS reduction of cytochrome *c* 24-fold above activity measured in the absence of CaM. As described above for citrulline formation and NADPH oxidation, the same relative ranking of the mutant CaMs was observed. The B3Q mutant supported nNOS cytochrome *c* reduction to 76%, and the B2Q and B4Q mutants supported greater than 50%, while the B1Q and B1234Q mutants activated to 11% of the wild-type CaM rate. The relative rates of NADPH oxidation in the presence of cytochrome *c* by both wild-type nNOS and the heme-deficient C415A mutant nNOS (*12*) are given in Table 3. NADPH oxidation by nNOS in control samples was found to be 150-fold faster when cytochrome *c* was present in the assay (Table 3) than

Table 2: nNOS Reduction of Cytochrome *c*

CaM	activity[a] (μmol min^{-1} mg^{-1})[b]	CaM	activity[a] (μmol min^{-1} mg^{-1})[b]
control	1.1 ± 0.2	B2Q	13.2 ± 1.3
bovine (WT)	25.5 ± 1.5	B3Q	20.1 ± 1.7
wild-type	26.4 ± 3.0	B4Q	13.9 ± 1.7
B1Q	3.0 ± 0.4	B1234Q	2.9 ± 0.6

[a] Assays contained nNOS (10−20 nM) and CaM (300 nM), as described under Experimental Procedures. [b] Values are the average of two or more experiments, each performed in duplicate. Errors are the standard error of the means. Control represents nNOS activity in the absence of CaM. Wild-type and B*x*Q CaMs are from *Drosophila*.

Table 3: NADPH Oxidation in the Presence of Cytochrome *c*

CaM	activity (nmol min^{-1} mg^{-1})[a]	
	wild-type nNOS[b]	C415A mutant nNOS[c]
control	1621.5 ± 218.1	779.1 ± 86.5
bovine (WT)	14441.0 ± 2026.6	8593.8 ± 1324.8
wild-type	15556.0 ± 881.1	10208.5 ± 40.3
B1Q	3016.7 ± 30.8	2292.7 ± 318.6
B2Q	10010.3 ± 1319.1	7094.7 ± 310.0
B3Q	14381.5 ± 225.6	7929.0 ± 225.5
B4Q	11548.5 ± 1376.7	6955.4 ± 31.3
B1234Q	2255.8 ± 223.5	1721.0 ± 65.1

[a] Values are the mean ± standard error of the mean of a representative experiment performed in duplicate. [b] Assays contained wild-type nNOS (8.2 nM) and CaM (150 nM) as described under Experimental Procedures. [c] Assays contained C415A mutant nNOS (9.2 nM) and CaM (150 nM) as described under Experimental Procedures. Control represents activity in the absence of CaM. Wild-type and B*x*Q CaMs are from *Drosophila*.

in its absence (Table 1). Unlike the 93-fold increase in the rate of NADPH oxidation obtained with wild-type CaM in the absence of cytochrome *c* (Table 1), only a 10-fold increase in that rate was obtained when cytochrome *c* was present (Table 3). The same ranking of the mutant CaMs described above was obtained for this activity. In the case of wild-type nNOS (containing heme), the B3Q mutant activated to 92%, the B2Q mutant to 64%, the B4Q mutant to 74%, the B1Q mutant to 19%, and the B1234Q mutant to 15% of the wild-type CaM rate (Table 3). Since in the absence of cytochrome *c* the C415A nNOS (lacking heme) was unable to oxidize NADPH at a measurable rate (data not shown) (*12*), its activity is only shown in the presence of cytochrome *c* (Table 3). C415A nNOS behaved similarly to wild-type nNOS under these conditions: wild-type CaM increased its reaction rate 13-fold; the B3Q mutant activated to 78%; B2Q and B4Q activated to similar levels (70% and 68% for B2Q and B4Q, respectively); the B1Q and B1234Q mutants caused the least activation, 23% and 17%, respectively.

Spectral Characterization of the Ferrous−CO Complex. The ability of the flavins to reduce the nNOS heme in the presence of each of the CaMs was determined spectrophotometrically by observing the formation of the ferrous−CO complex monitored at 443 nm. Complete formation of the complex was observed with all of the mutants as well as wild-type CaMs, although the time required for complete complex formation varied at 4 °C. The difference spectra in Figure 4 are representative of the changes observed over time. A decrease in absorbance at 400 nm occurs concomitantly with an increase at 443 nm. Changes in the α/β (500 nm − 600 nm) and δ (380 nm) regions can also be observed. In the case of bovine and *Drosophila* wild-type CaM,

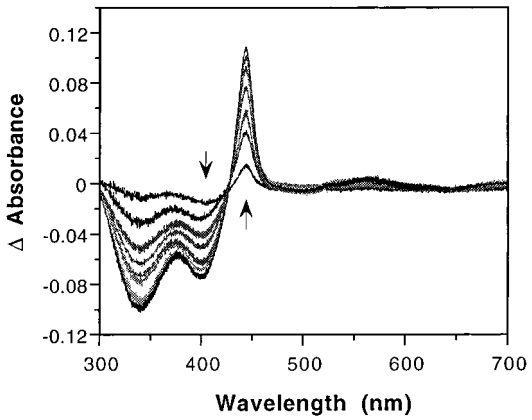

FIGURE 4: nNOS ferrous−CO difference spectra. Spectra of reduced CO-bound nNOS (1.88 μM) subtracted from an initial spectrum are shown. For this experiment, spectra were recorded as described under Experimental Procedures in the presence of NADPH (29.6 μM), $CaCl_2$ (1.25 mM), B1234Q mutant CaM (2.25 μM), and CO. As observed over time, the positive change in absorbance at 443 nm occurred concomitantly with the negative change at 400 nm. The initial spectrum was recorded 2 min after the addition of CaM, and each subsequent spectrum shown corresponds to that recorded at 10 min intervals.

complete formation of the complex was observed within 2 min (the earliest time at which spectra were recorded). The B3Q mutant also allowed complete formation of the ferrous−CO complex within 2 min. In the case of the B2Q and the B4Q mutants, complete formation of the complex was obtained approximately 16 min after the addition of these CaMs to the reaction. With the B1Q mutant, it took over 60 min for complete formation. The time required for complete complex formation was not affected by the addition of L-arginine (20 μM) (data not shown). Complex formation with the B1234Q mutant was similar to formation with the B1Q, requiring over 60 min. The difference spectra shown in Figure 4 are those obtained in the presence of the B1234Q mutant. The time-dependent changes are clearly visible, including the decrease at 340 nm, due to NADPH consumption. In the absence of CaM, formation of the ferrous−CO complex occurred at an observable rate only at 37 °C, and was significantly slower (10% formed after 10 min) than in the presence of any CaM mutant (50% formed after 10 min with the B1Q and B1234Q mutants at 4 °C). At 37 °C, complete formation of the complex was observed within 2 min for all CaMs examined.

To rule out the possibility that the mutant CaMs were affecting the binding of substrate to nNOS, the binding of L-arginine, in the presence or absence of CaM, was followed as a blue shift in the heme Soret (data not shown). K_d values between 0.1 and 0.6 μM were obtained in all cases. These values are in agreement with previously published values (*37*). The differences in nNOS activities measured with these CaMs, therefore, are not due to changes in the binding of substrate.

*Determinations of Binding Interaction*s. To determine whether the various *Drosophila* CaMs were binding to nNOS, their ability to inhibit the binding of bovine ^{125}I-CaM was measured. To ensure that CaM would remain bound to nNOS during the separation procedure, Ca^{2+} was included in all buffers. With the exception of the B1234Q mutant CaM, the relative binding affinities for the various CaMs obtained from the binding competition curves (Dixon plots) were all in the nanomolar range. Both bovine and wild-

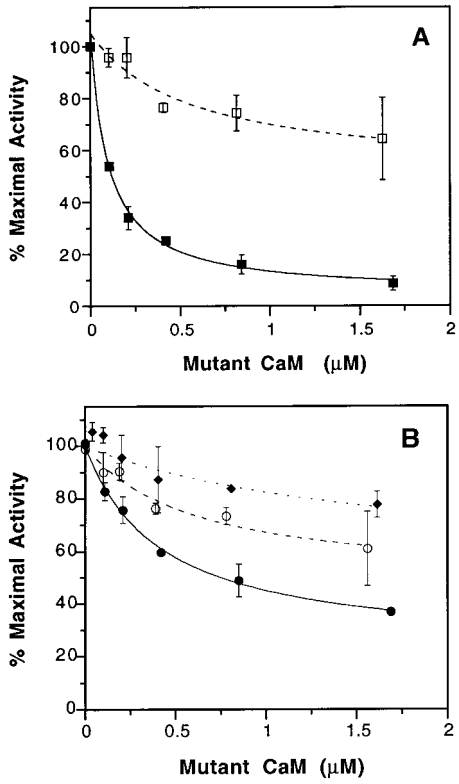

FIGURE 5: Inhibition of *Drosophila* wild-type CaM-mediated nNOS Activity. Activity was determined using the hemoglobin assay. Assays contained nNOS (36−40 nM), wild-type CaM (58.6 nM), $CaCl_2$ (1.2 mM), L-arginine (50 μM), H_4B (7.5 μM), DTT (100 μM), oxyhemoglobin (6 μM), NADPH (60 μM), and HEPES (100 mM, pH 7.5). Activity in the absence of mutant CaM represents maximal (100%) activity. Activities in the presence of mutant CaMs are given as a percent of the maximal activity. Data points are the average of two separate experiments; the error bars represent the standard deviation. Panel A shows inhibition of wild-type activity in the presence of B1Q mutant (■) and B1234Q mutant (□). Panel B shows inhibition of wild-type activity in the presence of B2Q mutant (●), B3Q mutant (◆), and B4Q mutant (○).

type CaM bound nNOS with affinities between 30 and 70 nM. The B1Q and B2Q mutants bound with lower affinity than wild-type (175−190 nM), and the B3Q and B4Q mutants bound with even lower affinities (300−500 nM). The B1234Q mutant was also found to bind to nNOS, but its affinity was between 6 and 10 μM.

We also examined the ability of each mutant CaM to inhibit wild-type CaM-mediated nNOS activity; these results are presented in Figure 5. The ability of mutant CaMs to inhibit nNOS activity provides an estimate of the mutant's ability to displace wild-type CaM from nNOS, and these results are consistent with the binding competition results discussed previously. The activity inhibition results, however, are best interpreted when comparing mutant CaMs with similar intrinsic abilities to activate nNOS. For example, the B1Q mutant was better able to displace wild-type CaM than the B1234Q mutant (Figure 5A), although they possess similar abilities to activate nNOS. The B1234Q mutant would, presumably, completely displace wild-type CaM, but concentrations required to do so were not feasible. Similarly, although the B2Q and B4Q mutants possess the same intrinsic nNOS activation capabilities, the B2Q mutant displaced wild-type CaM better than the B4Q mutant (Figure 5B). The B3Q mutant also displaced wild-type CaM from nNOS, but, as expected based on the activity obtained with the B3Q mutant alone (see Figure 3), 80% of nNOS activity remained (Figure 5B).

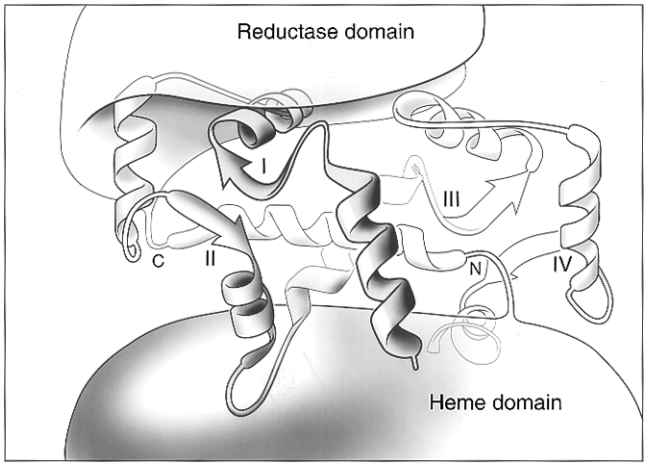

FIGURE 6: Schematic representation of possible nNOS interactions with CaM. The Roman numerals represent each of the Ca^{2+} binding sites of CaM. nNOS is shown as two separate domains: the reductase domain, which is located in the C-terminal half of the protein; and the heme domain, which is located in the N-terminal half, separated by the helical CaM binding sequence. The carboxy-terminus of the CaM binding sequence is indicated by the letter C, and the aminoterminus by the letter N. The structure of CaM and the helical segment of nNOS was adapted from the reported solution structure of CaM complexed with a peptide from MLCK (*38*). The latch domain is formed by residues of helix 2 (located immediately after site I) and helix 6 (located immediately after site III).

DISCUSSION

Although structural information about the full-length nNOS is not presently available, Zhang and colleagues (*18*) have demonstrated that the putative CaM binding sequence on nNOS interacts with CaM in an antiparallel orientation similarly to myosin light chain kinase (MLCK), that is, that the amino-terminal lobe of CaM (sites I and II) binds to the C-terminal end of the peptide sequence, and the carboxy-terminal lobe (sites III and IV) binds to the N-terminus. This structural representatation is depicted in Figure 6. The Ca^{2+}/CaM·peptide structure shown was derived from the NMR structure of Ca^{2+}/CaM complexed to the peptide corresponding to the CaM binding domain of skeletal muscle MLCK (*38*). This orientation of CaM in complexes with target peptides has been previously observed (*38*, *39*, *40*, *41*). The results presented in this study were used to further position the two domains of nNOS relative to the four Ca^{2+} binding sites of CaM. Namely, the data obtained with the B1Q mutant suggest that residues of site I of CaM interact with residues in the reductase domain of nNOS. This explains, then, why mutating site I of CaM affects all electron transfer reactions of nNOS to the same extent. Although Ca^{2+} binding site II of CaM is, like site I, located in the amino-terminal lobe, the results with the B2Q mutant suggest that this site does not directly influence the reductase domain. Instead, similarly to the site IV mutant (B4Q), it appears to affect heme domain functions. The effect of the site IV mutant on the heme-related activities was expected, however, given its assumed proximity to this domain. Lastly, mutating Ca^{2+} binding site III of CaM did not significantly affect any nNOS function, suggesting that this site may not directly interact with either domain.

We can conclude from our data that full activation of nNOS by CaM requires that all four Ca^{2+} binding sites have Ca^{2+} bound. Activities of nNOS with the B3Q mutant, for the most part, approached maximal values. The function that appeared to be affected the most by mutation of site III was oxidation of NADPH in the absence of cytochrome *c*: only 45% of maximal wild-type nNOS activity was measured with this mutant (Table 1). This result may suggest a problem in electron transfer to the flavins from NADPH. Transfer of electrons from the flavins to cytochrome *c*, which involves the same process, however, was not affected (Table 3). Further, since substrate oxidation with the B3Q mutant was comparable to that with wild-type CaM, electron transfer from NADPH to the flavins and then to the heme must not be affected. In the absence of substrate or another electron acceptor, the site III mutation is only affecting the ability of nNOS to consume NADPH, which may be the result of nNOS structural constraints.

Mutation of Ca^{2+} binding site I greatly influenced activity. Whether the activity being measured involved intramolecular or intermolecular electron transfer, only a small increase in the control rates was obtained with the B1Q mutant (Tables 1, 2, and 3). nNOS activity with this mutant was the same as with the four-site mutant (B1234Q). The B1Q mutant, however, binds nNOS with greater affinity and was better able to inhibit wild-type CaM-mediated nNOS activity (Figure 5A). The inability of the B1234Q mutant to fully activate nNOS could be ascribed to its low binding affinity; however, for the B1Q mutant, this is not the case. In fact, the B1Q mutant binds nNOS with greater affinity than the B3Q mutant. The effects obtained with the B1Q mutant could be attributed to the reduced ability of binding site I to bind Ca^{2+}. Cytochrome *c* reductase activity was measured with the B1Q mutant at Ca^{2+} concentrations ranging from 1 to 100 mM. Activity increased from 12% of wild-type at 1 mM Ca^{2+} to 38% at 50 mM Ca^{2+}, before leveling off (data not shown). Inhibition of cytochrome *c* reductase activity in the presence of wild-type CaM was observed above 10 mM Ca^{2+} (data not shown), which may explain why B1Q did not increase activity further. Since all electron transfer steps in nNOS are affected by the B1Q mutant, we conclude that specific residues of Ca^{2+} binding site I of CaM must interact with the reductase domain, which is required for all of these steps.

Several other investigations have addressed the role that specific regions of CaM play in the activation of nNOS. However, none have determined what steps in electron transfer are affected. Using trypsin fragments corresponding to the two individual lobes of CaM (see Figure 2 legend for description of the lobes), Persechini and colleagues (*42*) demonstrated that citrulline formation by nNOS was observed only when the amino-terminal lobe fragment was added to the assay. In a separate report, using engineered CaMs whereby the two lobes were either interchanged or switched, it was shown that only CaMs that contain the amino-terminal lobe residues were able to support nNOS activity (*43*). Recently, Su and colleagues (*44*) found that nNOS bound to CaM−troponin C chimeras was unable to form citrulline. Troponin C (TnC), although structurally homologous to CaM, possesses a different primary amino acid sequence: TnC does not bind to or activate nNOS. Although most of the chimeric CaMs had a reduced ability to activate nNOS, the CaMs with EF-hands 1 or 3 of TnC were completely inactive, although they were found to bind to nNOS (*44*). Based on these results, Su and colleagues (*44*) have suggested a role for the latch domain of CaM in nNOS activation (see Figure 6 and legend). This latch has been proposed to form between residues of helix 2 and helix 6 of CaM, when it binds to a target peptide (*40*). Our results with the B1Q mutant support a role for helix 2 of the latch domain in nNOS activation. The mutation of Ca^{2+} binding site I of CaM, since located at the beginning of helix 2 (see Figure 2), may affect the structure or positioning of helix 2 in such a way that the latch may not be able to form. By a similar argument, the site III mutation, which affects helix 6, would be expected to have an altered ability to form the latch domain, and thus give poor nNOS activation. Our finding that the B3Q mutant is a good activator of nNOS appears to contradict the role of helix 6 and the latch domain in the activation, as suggested by Su and colleagues (*44*). It is conceivable that the effects of the site III mutation on the structure of CaM are compensated for upon B3Q binding to nNOS. Mukherjea and Beckingham (*45*) have shown that B3Q is the only Q series mutant that forms a complex similar to wild-type CaM with the model target peptide mastoparan. The investigations discussed previously have demonstrated the importance of the amino-terminal lobe of CaM for nNOS activity. The present study provides a possible explanation for their findings, in that it demonstrates that the effects on catalytic activity they have observed could be due to the influence of site I on the reductase domain of nNOS.

The activity of nNOS in the presence of the site II mutant CaM (B2Q) was, for the most part, indistinguishable from the activity in the presence of the site IV mutant (B4Q). The relative rates for all activities measured with these two mutants were faster than those with the B1Q mutant and slower than those with the B3Q mutant. However, with these two mutants, cytochrome *c* mediated activities were affected to a lesser extent than activities dependent on the nNOS heme. Oxidation of NADPH serves as the best example. In the absence of cytochrome *c*, nNOS oxidizes NADPH at a rate that was 15% of maximal, with either B2Q or B4Q (Table 1). In the absence of cytochrome *c* (see Scheme 1), this function is dependent on the ability of the nNOS heme to accept electrons from the flavins, followed by reoxidation of the heme by O_2. Cytochrome *c* increased NADPH oxidase activity with the B2Q and B4Q mutants to levels obtained with the B3Q mutant. Greater than 64% of wild-type CaM activity was measured, again suggesting that these mutations do not directly affect the flavin's ability to accept electrons from NADPH. However, the ability of the flavins to transfer electrons to the nNOS heme seems to be hampered by either of these two mutations. Citrulline formation was measured between 25% and 30% of maximal. Whereas the results with the B1Q mutant suggest that this region of CaM affects the orientation of the reductase domain of nNOS, the results with the B2Q and B4Q mutants suggest that these sites affect primarily the nNOS heme domain. Since site IV is located in the carboxy-terminal lobe of CaM, we expected that the B4Q mutant would affect the heme domain. It was harder to envision how the B2Q mutant, located in the amino-terminal lobe of CaM, could have the same effect. Figure 6 shows a possible way that the mutations of sites II and IV of CaM could both affect the heme domain. Basically, when nNOS binds CaM, the heme domain could straddle across the CaM molecule in such a way that it would

contact both helices 4 and 8 of CaM (we expect that helix 4 would be affected by the mutation of site II, and helix 8 by the mutation of site IV).

The binding affinities of the various CaM mutants for nNOS could be ruled out as a possible explanation for the observed differential activities. In the case of the site IV mutant, the weakened affinity of B4Q may explain its reduced ability to activate nNOS. A recent report by George and colleagues (*46*) showed that replacing the residues of helix 7 of CaM with those of TnC resulted in 50% loss of maximal nNOS activity. They attributed the loss of activity to a reduced ability of this mutant CaM to bind nNOS, since many of the necessary CaM binding contacts reside in this region. Mutating site IV may affect the orientation of critical nNOS contact regions of CaM since helix 7 is associated with this site (see Figure 2). Binding inhibition results, in fact, show that the B4Q mutant has a weakened affinity for nNOS than the other mutant CaMs. However, if the inability of the mutant CaMs to fully activate nNOS was simply a function of binding affinity, then we would have expected that activity would increase as a function of CaM concentration. This was not the case for any of these mutant CaMs, since activity reached a maximum for each that was lower than the maximal activity expected (Figure 3). The activity of nNOS with the B2Q mutant cannot be explained as a function of binding affinity, since this mutant CaM binds nNOS with greater affinity than the more active B3Q mutant. Furthermore, the site III mutant (B3Q), which activates to levels that approximate those of wild-type CaM, binds nNOS with lower affinity than the site I mutant (B1Q), which is a poor activator. It appears, therefore, that in addition to the conventional interactions between CaM and the putative CaM binding sequence on nNOS there are other critical contacts which are required to allow catalysis.

A recent report by Gachhui and co-workers (*36*) has suggested that CaM's actions on nNOS are completely within the reductase domain. The present findings demonstrate that CaM influences the heme domain as well. The hypothesized interactions between CaM and nNOS given in Figure 6 present one possible explanation for the data obtained with the Ca^{2+} binding site mutants studied. Figure 6 also shows how CaM could affect both reductase and heme domains of nNOS. Further structural and activity studies are necessary to fully understand the molecular details of CaM regulation of NOS activity.

ACKNOWLEDGMENT

We thank the members of both research groups for help provided during the time the experiments were being conducted as well as for their helpful suggestions during the preparation of the manuscript. Special thanks are also due to Sami Mahrus (Marletta laboratory) for supplying samples of the purified C415A mutant nNOS, and to various members of the Beckingham laboratory including Dai-rong Su, Poushali Mukherjea, and Aaron Castonell, who supplied purified *Drosophila* calmodulins.

REFERENCES

1. Stuehr, D. J., Kwon, N. S., Nathan, C. F., Griffith, O. W., Feldman, P. L., and Wiseman, J. (1991) *J. Biol. Chem. 266*, 6259−6263.
2. Pufahl, R. A., Nanjappan, P. G., Woodard, R. W., and Marletta, M. A. (1992) *Biochemistry 31*, 6822−6828.
3. Klatt, P., Schmidt, K., Uray, G., and Mayer, B. (1993) *J. Biol. Chem. 268*, 14781−14787.
4. Cho, H. J., Xie, Q.-W., Calaycay, J., Mumford, R. A., Swiderek, K. M., Lee, T. D., and Nathan, C. (1992) *J. Exp. Med. 176*, 599−604.
5. McMillan, K., Bredt, D. S., Hirsch, D. J., Snyder, S. H., Clark, J. E., and Masters, B. S. S. (1992) *Proc. Natl. Acad. Sci. U.S.A. 89*, 11141−11145.
6. Stuehr, D. J., and Ikeda-Saito, M. (1992) *J. Biol. Chem. 267*, 20547−20550.
7. White, K. A., and Marletta, M. A. (1992) *Biochemistry 31*, 6627−6631.
8. Hevel, J. M., White, K. A., and Marletta, M. A. (1991) *J. Biol. Chem. 266*, 22789−22791.
9. Mayer, B., John, M., Heinzel, B., Werner, E. R., Wachter, H., Schultz, G., and Böhme, E. (1991) *FEBS Lett. 288*, 187−191.
10. Stuehr, D. J., Cho, H. J., Kwon, N. S., Weise, M. F., and Nathan, C. F. (1991) *Proc. Natl. Acad. Sci. U.S.A. 88*, 7773−7777.
11. Hevel, J. M., and Marletta, M. A. (1992) *Biochemistry 31*, 7160−7165.
12. Richards, M. K., Clague, M. J., and Marletta, M. A. (1996) *Biochemistry 35*, 7772−7780.
13. Bredt, D. S., Hwang, P. M., Glatt, C. E., Lowenstein, C., Reed, R. R., and Snyder, S. H. (1991) *Nature (London) 351*, 714−718.
14. McMillan, K., and Masters, B. S. S. (1995) *Biochemistry 34*, 3686−3693.
15. Richards, M. K., and Marletta, M. A. (1994) *Biochemistry 33*, 14723−14732.
16. Vorherr, T., Knopfel, L., Hofmann, F., Mollner, S., Pfeuffer, T., and Carafoli, E. (1993) *Biochemistry 32*, 6081−6088.
17. Zhang, M., and Vogel, H. J. (1994) *J. Biol. Chem. 269*, 981−985.
18. Zhang, M., Yuan, T., Aramani, J. M., and Vogel, H. J. (1995) *J. Biol. Chem. 270*, 20901−20907.
19. Sheta, E. A., McMillan, K., and Masters, B. S. S. (1994) *J. Biol. Chem. 269*, 15147−15153.
20. Abu-Soud, H. M., and Stuehr, D. J. (1993) *Proc. Natl. Acad. Sci. U.S.A. 90*, 10769−10772.
21. Abu-Soud, H. M., Yoho, L. L., and Stuehr, D. J. (1994) *J. Biol. Chem. 269*, 32047−32050.
22. Crivici, A., and Ikura, M. (1995) *Annu. Rev. Biophys. Biomol. Struct. 24*, 85−116.
23. Vogel, H. J., and Zhang, M. (1995) *Mol. Cell. Biochem. 149/150*, 3−15.
24. Babu, Y. S., Sack, J. S., Greenhough, T. J., Bugg, C. E., Means, A. R., and Cook, W. J. (1985) *Nature 315*, 37−40.
25. Taylor, D., Sack, J. S., Maune, J. F., Beckingham, K., and Quiocho, F. A. (1991) *J. Biol. Chem. 266*, 21375−21380.
26. Persechini, A., and Kretsinger, R. H. (1988) *J. Biol. Chem. 263*, 12175−12178.
27. Ikura, M., Hiraoki, T., Hikichi, K., Mikuni, T., Yazawa, M., and Yagi, K. (1983) *Biochemistry 22*, 2573−2579.
28. Ikura, M., Hiraoki, T., Hikichi, K., Minowa, O., Yamaguchi, H., Yazawa, M., and Yagi, K. (1984) *Biochemistry 23*, 3124−3128.
29. Maune, J. F., Klee, C. B., and Beckingham, K. (1992) *J. Biol. Chem. 267*, 5286−5295.
30. Gao, H. Z., Krebs, J., VanBerkum, M. F. A., Tang, W.-J., Maune, J. F., Means, A. R., Stull, J. T., and Beckingham, K. (1993) *J. Biol. Chem. 268*, 20096−20104.
31. GuptaRoy, B., Beckingham, K., and Griffith, L. C. (1996) *J. Biol. Chem. 271*, 19846−19851.
32. Mukherjea, P., Maune, J. F., and Beckingham, K. (1996) *Protein Sci. 5*, 468−477.
33. Hevel, J. M., and Marletta, M. A. (1994) *Methods Enzymol. 233*, 250−258.
34. Stevens-Truss, R., and Marletta, M. A. (1995) *Biochemistry 34*, 15638−15645.
35. Hurshman, A. R., and Marletta, M. A. (1995) *Biochemistry 34*, 5627−5634.

36. Gachhui, R., Presta, A., Bentley, D. F., Abu-Soud, H. M., McArthur, R., Brudvig, G., Ghosh, D. K., and Stuehr, D. J. (1996) *J. Biol. Chem. 271*, 20594−20602.
37. Matsouka, A., Stuehr, D. J., Olson, J. S., Clark, P., and Ikeda-Saito, M. (1994) *J. Biol. Chem. 269*, 20335−20339.
38. Ikura, M., Clore, G. M., Gronenborn, A. M., Zhu, G., Klee, C. B., and Bax, A. (1992) *Science 256*, 632−638.
39. Ikura, M., Kay, L. E., Krinks, M., and Bax, A. (1991) *Biochemistry 30*, 5498−5504.
40. Meador, W. E., Means, A. R., and Quiocho, F. A. (1992) *Science 257*, 1251−1255.
41. Meador, W. E., Means, A. R., and Quiocho, F. A. (1993) *Science 262*, 1718−1721.
42. Persechini, A., McMillan, K., and Leaky, P. (1994) *J. Biol. Chem. 269*, 16148−16154.
43. Persechini, A., Gansz, K. J., and Paresi, R. J. (1996) *Biochemistry 35*, 224−228.
44. Su, Z., Blazing, M. A., Fan, D., and George, S. E. (1995) *J. Biol. Chem. 270*, 29117−29122.
45. Mukherjea, P., and Beckingham, K. (1993) *Biochem. Mol. Biol Int. 29*, 555−563.
46. George, S. E., Su, Z., Fan, D., Wang, S., and Johnson, D. J. (1996) *Biochemistry 35*, 8307−8313.

BI970973K